Oxidation of Metals, Vol. 25, Nos. 5/6, 1986

Selective Oxidation of FeCr Alloys in the 295–450 K Temperature Range

Gunnar Hultquist,* Masahiro Seo,† and Norio Sato†

Received July 25, 1985; revised October 31, 1985

A series of iron-chromium alloys were oxidized for 10^2 to 6×10^4 s in air and in the 295–500 K temperature range. Room-temperature oxidation of iron, chromium, antimony, and copper were also conducted at extended times. Oxidation characteristics such as oxide thickness and composition of the oxide and of the underlying alloy were evaluated from measurements by electron spectroscopy for chemical analysis (ESCA). An initial selective oxidation of chromium with a concomitant chromium depletion in the alloy was found. This initial oxidation step is followed by growth of an outer, iron rich oxide which causes the former chromium depletion to vanish. Apparent activation energies extracted from parabolic oxidation kinetics (295–500 K) of the investigated metals were found to be in the 10–20 kcal/mole range.

KEY WORDS: selective oxidation; ESCA analysis; Fe–Cr alloys; oxidation kinetics; chromium depletion.

INTRODUCTION

The oxidation resistance of iron-chromium alloys is known to depend on the formation of chromium-rich oxides. While most studies on dry oxidation of these alloys have been conducted at temperatures >1000 K, Hultquist and Leygraf[1,2] have reported investigations at temperatures $700 < T < 850$, and recently, a study by Seo *et al.*[3] parallel to the present work has been carried out. Studies on oxidation of pure iron in the temperature range 300–500 K have been done,[4–6] but information on the oxidation kinetics of

*Department of Physical Chemistry, The Royal Institute of Technology, S-100 44 Stockholm, Sweden.
†Department of Engineering Science, Faculty of Engineering, Hokkaido University, Kita-13 Jo, Nishi-8 Chome Kita-ku, Sapporo 060, Japan.

0030-770X/86/0600-0363$05.00/0

Table I. Metals and Alloys Used in this Study

Metal/alloy (at.% Cr)	Approx. grain size (μm)
Fe	100
Fe9Cr	50
Fe15Cr	100
Fe50Cr	100
Cr	?
Cu	100
Sb	Single crystal

iron-chromium alloys at these low temperatures seems to be lacking. A better understanding of near-room-temperature dry oxidation might be useful, both to illuminate the general features involved in dry oxidation of iron-chromium alloys and for insight into wet oxidation (corrosion) of these alloys.

EXPERIMENTAL PROCEDURE

Specimen Preparation and Surface Oxidation

Metals and alloys used in this study are found in Table I, in which approximate grain sizes are indicated. The nominal bulk compositions of the alloys were checked in a scanning electron microscope with associated wavelength and X-ray spectrometers. From this analysis, nominal chemical compositions in Table I of the alloys should be accurate within 1%. All specimens used in this work were prepared by mechanical polishing. Prior to oxidation the specimens were polished with 1 μm diamond paste in ethanol, rinsed in ethanol, and dried for a few seconds in hot (330 K) air. Thermal oxidation was conducted in air in an ordinary oven ($\pm$5 K). The relative humidity was 40-60% during room temperature oxidation.

Surface Analysis

Electron spectroscopy for chemical analysis (ESCA) is a surface sensitive technique with a sampling depth in the nm range.[7] Basically, photoelectrons are emitted from a sample upon radiation of X-rays. In an electron energy analyzer a distribution of kinetic energies among the emitted electrons allows the identification of discrete peaks from all elements (except hydrogen) in the sample. The limit of detection is often in the 0.1-0.5 at.% range. It is also possible to separate the photoelectron peaks originating from elements in different valence states. Hence a quantification of both

oxidized and unoxidized chromium and iron can be done when using appropriate standards. If we assume the oxidized metal and alloy components to exist in an overlayer, we can extract the oxide thickness in ESCA. (This assumption is most reasonable in the present study of thermal oxidation at low temperautures.) For details of the surface sensitivity of ESCA and evaluation of thickness of an overlayer, see the experimental method in ref. 8.

In this study an ESCA spectrometer, Leybold-Heraeus 2000, was used to evaluate the chemical compositions and oxide thicknesses of the different metal and alloy surfaces subjected to thermal oxidation. AlK_α radiation was used for excitation of the photoelectrons. Quantification of the surface compositions was based on $Cu(2p_{3/2})$, $Fe(2p_{3/2})$, $Cr(2p_{3/2})$, and $Sb(3d_{5/2})$ lines using iron and chromium metals and thermally grown oxides as standards when evaluating the compositions of the iron-chromium alloys. The absolute accuracy in the results of the ESCA measurements of the alloys is believed to fall within 5 at.%, while the relative accuracy (comparisons of surface compositions between different alloys and oxidation runs) are probably within 2 at.%.

A mean free path of detected photoelectrons has been assumed to equal 1.5 nm. A change of the angle between surface and electron detector (take-off angle) from 90° to 30° was conducted in the analysis presented in Table V, giving an increase in surface sensitivity from 1.5 to 0.75 nm.

Definition of an Effective Diffusivity

It is of interest to describe the parabolic oxidation kinetics in terms of a corresponding diffusivity. If we approximate a diffusion length to equal half the existing oxide thickness, we can compare diffusivity in the metal (alloy) with the effective diffusivity during subsequent oxidation. The factor of one-half is due to an approximation of cation density (number/volume unit) being half in the oxide relative to the metal (alloy). Hence such a diffusivity, $D^{1/2} = d/2t^{1/2}$, where d equals the oxide thickness, and t equals the time of oxidation, is defined by parabolic oxidation kinetics. This definition of diffusivity is used in Fig. 6.

EXPERIMENTAL RESULTS

Thermal oxidation runs for certain times and temperatures produced metal and alloy surfaces, which were characterized by ESCA. This analysis gave data on chromium contents in oxides and underlying alloys as well as oxide thicknesses of the different samples. Hence in Table II the atomic ratios of oxidized chromium $[Cr/(Cr+Fe)]_{ox}$ after different times and temperatures of oxidation are presented. In the same manner the atomic

Table II. Atomic Ratios of Oxidized Chromium at Different Times and Temperatures in Fe9Cr, Fe15Cr, and Fe50Cr as Measured by ESCA

Time (s)	Temperature (K) 295	375	425	475	Alloy
100	14.9				Fe9Cr
100	25.6				Fe15Cr
100	79.1				Fe50Cr
1320	15.2	9.4	4.5	1.2	Fe9Cr
1320	25.8	19.1	7.8	2.6	Fe15Cr
1320	78.2	69.8	60.5	52.3	Fe50Cr
6000	13.9	7.2	2.7	0.6	Fe9Cr
6000	24.4	14.0	4.5	1.9	Fe15Cr
6000	78.5	64.3	53.8	48.6	Fe50Cr
64,800	13.7	3.9	0.9	0.8	Fe9Cr
64,800	23.1	9.1	3.0	1.2	Fe15Cr
64,800	78.0	61.7	52.4	43.8	Fe50Cr

ratios of metallic chromium $[Cr/(Cr+Fe)]_{me}$ from the ESCA analysis are shown in Table III. Due to the limited information depth in the surface analysis, these data could be obtained only when the thickness of the oxide was less than $\sim 2.5 \times$ the mean free path of detected electrons (3.8 nm with

Table III. Atomic Ratios of Metallic Chromium in Alloy beneath the Oxide, as Measured by ESCA after Oxidation at Different Times and Temperatures for Fe9Cr, Fe15Cr, and Fe50Cr.

Time (s)	Temperature (K) 295	375	425	475	Alloy
100	6.4				Fe9Cr
100	11.9				Fe15Cr
100	38.6				Fe50Cr
1320	7.5	8.5	9.9		Fe9Cr
1320	13.8	15.0	16.4		Fe15Cr
1320	40.2	43.1	47.1	49.2	Fe50Cr
6000	8.3	9.8	10.5		Fe9Cr
6000	14.0	15.1	17.0		Fe15Cr
6000	40.2	44.7	46.0	49.3	Fe50Cr
64,800	7.8	9.4			Fe9Cr
64,800	15.3	16.2			Fe15Cr
64,800	41.5	43.3	45.5	44.8	Fe50Cr

Table IV. Thickness of Oxide in nm as Measured by ESCA after Oxidztion at Different Times and Temperatures of Fe9Cr, Fe15Cr, and Fe50Cr

Time (s)	Temperature (K) 295	375	425	475	Alloy
100	0.71				Fe
100	0.71				Fe9Cr
100	0.69				Fe15Cr
100	0.65				Fe50Cr
100					Cr
1320	0.74	1.32	2.42	>4.5	Fe
1320	0.83	1.58	3.15	>4.5	Fe9Cr
1320	0.77	1.55	2.93	>4.5	Fe15Cr
1320	0.69	0.9	1.14	1.46	Fe50Cr
1320			1.22	1.28	Cr
6000	0.75	1.46	3.51	>4.5	Fe
6000	1.04	2.10	3.90	>4.5	Fe9Cr
6000	0.89	1.86	3.68	>4.5	Fe15Cr
6000	0.83	0.99	1.35	1.82	Fe50Cr
6000					Cr
64,800	0.98	2.30	>4.5	>4.5	Fe
64,800	1.02	2.97	>4.5	>4.5	Fe9Cr
64,800	1.08	2.85	>4.5	>4.5	Fe15Cr
64,800	0.81	1.08	1.58	2.54	Fe50Cr
64,800			1.50	1.79	Cr

$\lambda = 1.5$ nm). This restriction is naturally present also in Table IV, where thicknesses of the oxides produced during oxidation of the alloys are shown. Combinations of the results in Tables II, III, and IV are seen in the Figs. 1, 2, and 3. To find the time of oxidation for a certain alloy and temperature in the figures we need to consult one of the tables. The reason to make a combination of the data in Tables II, III, and IV is to reveal a general pattern. Hence in Figs. 1, 2, and 3 is seen that a certain alloy surface composition, chromium in oxide = Cr in ox. state = $[Cr/(Cr+Fe)]_{ox}$ and chromium in underlying alloy = Cr in met. state = $[Cr/(Cr+Fe)]_{me}$, can be correlated to a unique oxide thickness irrespective of time and temperature of oxidation.

Extended times of exposure at room temperature of iron and chromium, as well as copper and antimony for comparison purposes, have been carried out. Again, assuming the mean free path $\lambda = 1.5$ nm, the thicknesses vs square root of exposure time are seen in Fig. 4. The oxide growth follows

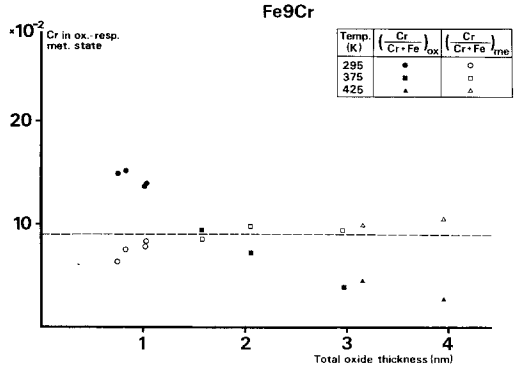

Fig. 1. Chromium surface content; chromium in oxidized state, $[Cr/(Cr+Fe)]_{ox}$; and chromium in metallic state, $[Cr/(Cr+Fe)]_{me}$; vs. total oxide thickness of Fe9Cr.

a parabolic behavior pattern on these metals except for the very initial oxidation stage as can be inferred from this figure. Oxidation at elevated temperatures of copper, iron, and chromium (Fig. 5 and Table IV) also gave reasonable parabolic oxide growth, thereby causing an effective (or apparent) diffusivity (see above). Such diffusivities are shown in Fig. 6.

DISCUSSION

The initial oxidation (oxide thickness <0.5 nm), which takes place more or less instantly, is faster on pure chromium than on pure iron as can be seen in the extrapolation towards zero time in Fig. 4. Hence, it is

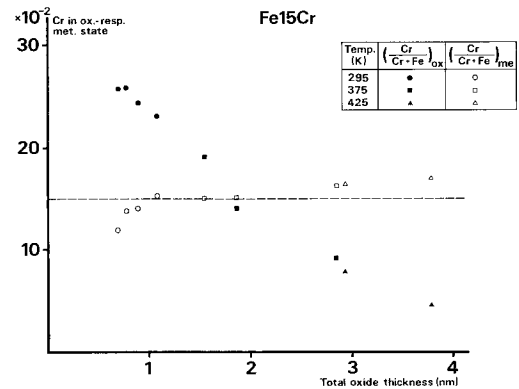

Fig. 2. Same as Fig. 1 for Fe15Cr.

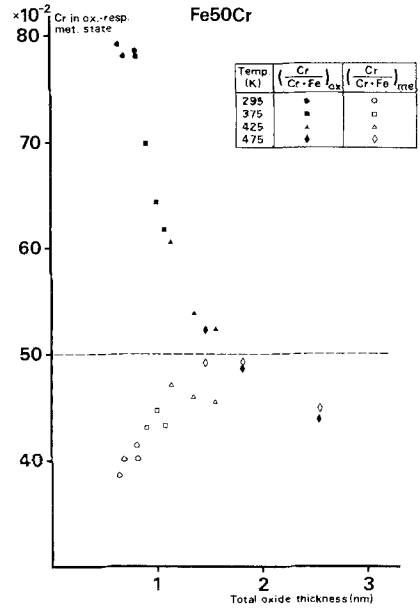

Fig. 3. Same as Fig. 1 for Fe50Cr.

reasonable that we also find chromium enrichment in the instantly (polished in ethanol + 100 s in air) formed oxide. This enrichment is most clear when we inspect Fig. 3, where a chromium content close to 80 at.% on the Fe50Cr alloy is found. In an earlier study on oxidation of an Fe18Cr2Mo alloy at low oxygen partial pressures, sticking probabilities of chromium and iron were evaluated.[2] From this study we expect the amount of oxidized iron to equal ~15% of oxidized chromium if the supply of iron and chromium is

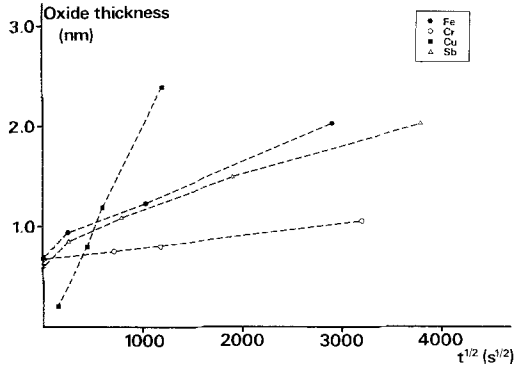

Fig. 4. Room-temperature oxidation in air of some metals, 1 μm mech. pol. in ethanol, ESCA, $\lambda = 1.5$ nm.

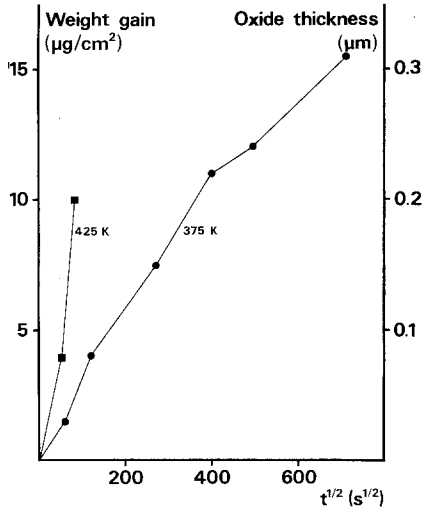

Fig. 5. Weight gain and average thickness of Cu_2O in air oxidation of copper.

equal and the supply of oxygen (determined by oxygen partial pressure) is far more than the supply of iron and chromium. In the alloy Fe50Cr this would give a chromium content of 87%: $100 \times 50/(50+0.15 \times 50)$. The values for Fe9Cr and Fe15Cr should be 40% and 54%, respectively. In Figs. 1, 2, and 3 these values might be found by extrapolating down to a total oxide thickness of a monolayer of 0.3 nm. Only oxide growth corresponding to that thickness guarantees the "supply" of chromium and iron corresponding to the alloy composition.

Continued oxidation causes the supply of chromium to be lowered due to the depletion in chromium in the alloy region beneath the oxide film. In

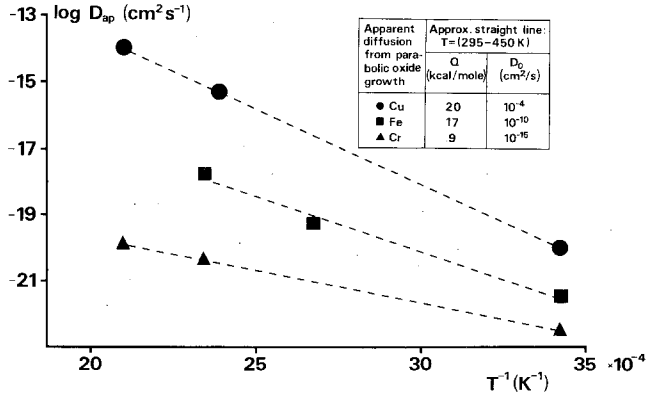

Fig. 6. Apparent diffusion from parabolic oxidation in air.

Figs. 1-3 we observe a decreasing chromium content in the oxide while the chromium depletion in the alloy region is lowered and is not significant at oxide thicknesses $\lesssim 2$ nm.

In Table V, results are presented of chromium contents from measurements where the surface sensitivity is increased (see Experimental Procedure). We observe a concentration gradient of chromium with the highest concentration of chromium at the oxide/alloy interface. In fact, the "profiles" of chromium contents in the oxides, $[Cr/(Cr+Fe)]_{ox}$, in Figs. 1-3 can be seen as depth profiles (with zero equal oxide/metal interface) if we assume that the oxidation takes place entirely at the oxide/gas interface.

In Fig. 4, where the oxide thickness is plotted vs square root of oxidation time, iron and chromium do not obey a parabolic growth during the initial oxidation, as already discussed. However, when the oxide grows thicker ($\lesssim 1$ nm) more of its intrinsic transport properties will determine the further growth, especially if no structural changes occur during the oxidation. More or less straight lines (parabolic growth) are also found in Fig. 4 when the oxide thickness exceeds $\lesssim 1$ nm. In oxidation of the alloys, changes in oxide composition take place during the oxidation. This makes a parabolic oxide growth less probable since the transport properties may change during oxidation due to the changes in composition of the oxide.

One feature in Fig. 6 is considerably lower oxidation rates (apparent diffusivity) for chromium compared with both copper and iron. Apparent activation energies found from the slopes in Fig. 6 are significantly lower than activation energies found in high-temperature (>1000 K) studies on inter-diffusion and self-diffusion. Hultquist has predicted that activation energies in the range 10–25 kcal/mole should be found for low-temperature ($\lesssim 500$ K) diffusion in polycrystalline materials.[9] Then we might expect also to find these numerical values as apparent activation energies for parabolic oxidation kinetics where diffusion of oxygen and cations are rate determining for the oxidation.

Table V. Chromium Content in the Oxidized State[a] Measured at two Different Surface Sensitivities

Alloy	Oxidation		Mean information depth	
	Times (s)	Temperatures (K)	1.5 nm	0.75 nm
Fe50Cr	8.6×10^4	293	0.78	0.75
Fe50Cr	1.8×10^3	423	0.66	0.56
Fe15Cr	1.2×10^3	373	0.19	0.16

[a] $[Cr/(Cr+Fe)]_{ox}$.

CONCLUSIONS

The following conclusions are drawn from the present study of air oxidation of iron-chromium alloys in the 295–500 K temperature range:

1. The initial oxidation step ($\lesssim$0.3 nm) is faster on chromium than on iron.
2. A selective intial oxidation takes place on iron-chromium alloys in analogy with 1.
3. As a consequence of 2, a depletion of chromium is created in the alloy region immediately beneath the oxide.
4. Oxidation following the initial oxidation in 1 is characterized by growth of an iron rich oxide at the oxide-gas interface.
5. As a consequence of 4, the depletion in chromium is lowered and not significant after extended times of oxidation.
6. The parabolic oxidation of copper, iron, and chromium gives apparent diffusion constants and activation energies near room temperature: Cu, 10^{-20} cm^2 s^{-1} and 20 kcal/mole; Fe, 10^{-21} cm^2 s^{-1} and 17 kcal/mole; Cr, 5×10^{-23} cm^2 s^{-1} and 9 kcal/mole.

ACKNOWLEDGMENTS

This work was conducted in a Japan-Sweden collaborative research project supported by JSPS (Japan Society of Promotion of Science). The authors wish to acknowledge the financial support of JSPS and are much indebted to Dr. C. Leygraf and Prof. E. Mattsson at the Swedish Corrosion Institute and Prof. J. C. Eriksson at the Royal Institute of Technology for their cooperation in conducting the collaborative research. Financial support from NFR (Swedish Natural Science Research Council) is gratefully acknowledged.

REFERENCES

1. C. Leygraf and G. Hultquist, *Surf. Sci.* **61**, 69 (1976).
2. G. Hultquist and C. Leygraf, *Corr. Sci.* **22**, 331 (1982).
3. M. Seo, G. Hultquist, F. Baba, and N. Sato, *Oxid. Met.* (to be published).
4. J. Kruger and H. T. Yolhen, *Corr.* **20**, 291 (1964).
5. P. B. Swell and M. Cohen, *J. Electrochem. Soc.* **111**, 501 (1964).
6. S. I. Ali and G. C. Wood, *Br. Corr. J.* **4**, 133 (1969).
7. T. A. Carlson, *Photoelectron and Auger Spectroscopy* (Plenum Press, New York, 1975).
8. G. Hultquist and H. Herø, *Corr. Sci.* **24**, 789 (1984).
9. G. Hultquist, *Mat. Sci.* (to be published).